Natural Heteroplasmy and Mitochondrial Inheritance in Bivalve Molluscs

Natural Heteroplasmy and Mitochondrial Inheritance in Bivalve Molluscs

Journal:	*Integrative and Comparative Biology*
Manuscript ID	ICB-2019-0088.R1
Manuscript Type:	Symposium article
Date Submitted by the Author:	n/a

Complete List of Authors:	Ghiselli, Fabrizio; University of Bologna, Biological, Geological, and Environmental Sciences Maurizii, Maria Gabriella; University of Bologna, Department of Biological, Geological and Environmental Sciences (BiGeA) Reunov, Arkadiy; Russian Academy of Sciences Far Eastern Branch Ariño Bassols, Helena; Universitat de Barcelona, Departament de Fisiologia i Immunologia Cifaldi, Carmine; University of Bologna, Department of Biological, Geological and Environmental Sciences (BiGeA) Pecci, Andrea; University of Bologna, Department of Biological, Geological and Environmental Sciences (BiGeA) Aleksandrova, Yana; Russian Academy of Sciences Far Eastern Branch Bettini, Simone; University of Bologna, Department of Biological, Geological and Environmental Sciences (BiGeA) Passamonti, Marco; University of Bologna, Department of Biological, Geological and Environmental Sciences (BiGeA) Franceschini, Valeria; University of Bologna, Department of Biological, Geological and Environmental Sciences (BiGeA) Milani, Liliana; University of Bologna, Department of Biological, Geological and Environmental Sciences (BiGeA)

Keywords:	mitochondrial heteroplasmy, doubly uniparental inheritance of mitochondria (DUI), Ruditapes philippinarum, germline, immunohistochemistry, OXPHOS

Natural Heteroplasmy and Mitochondrial Inheritance in Bivalve Molluscs

*Fabrizio Ghiselli[1#], Maria Gabriella Maurizii[1#], Arkadiy Reunov[2], Helena Ariño[3], Carmine Cifaldi[1], Andrea Pecci[1], Yana Alexandrova[2], Simone Bettini[1], Marco Passamonti[1], Valeria Franceschini[1], Liliana Milani[1]**

[1]Department of Biological, Geological and Environmental Sciences (BiGeA), University of Bologna, 40126, Bologna, Italy

[2]National Scientific Centre of Marine Biology, Russian Academy of Sciences Far Eastern Branch, 690041, Vladivostok, Russia

[3]Departamento de Fisiología e Inmunología, Universitat de Barcelona, 08028, Barcelona, Spain

[#] *Equal contribution*

Author for correspondence

*liliana.milani@unibo.it

Running Title: Natural heteroplasmy in bivalves

Total number of words: 7,354

Abstract

Heteroplasmy is the presence of more than one type of mitochondrial genome within an individual, a condition commonly reported as unfavourable and affecting mitonuclear interactions. So far, no study has investigated heteroplasmy at protein level, and whether it occurs within tissues, cells, or even organelles.

The only known evolutionarily stable and natural heteroplasmic system in Metazoa is the Doubly Uniparental Inheritance (DUI)—reported so far in ~100 bivalve species—in which two mitochondrial lineages are present: one transmitted through eggs (F-type) and the other through sperm (M-type). Because of such segregation, mitochondrial OXPHOS proteins reach a high amino acid sequence divergence (up to 52%) between the two lineages in the same species. Natural heteroplasmy coupled with high sequence divergence between F- and M-type proteins provides a unique opportunity to study their expression and assess level and extent of heteroplasmy. Here, for the first time, we immunolocalized F- and M-type variants of three mitochondrially-encoded proteins in the DUI species *Ruditapes philippinarum*, in germline and somatic tissues at different developmental stages. We found heteroplasmy at organelle level in undifferentiated germ cells of both sexes, and in male soma, while gametes were homoplasmic: eggs for the F-type and sperm for the M-type. Thus, during gametogenesis only the sex-specific mitochondrial variant is maintained, likely due to a process of meiotic drive. We examine the implications of our results for DUI proposing a revised model, and we discuss interactions of mitochondria with germ plasm and their role in germline development. Molecular and phylogenetic evidence suggests that DUI evolved from the common strictly maternal inheritance, so the two systems likely share the same underlying molecular mechanism, making DUI a useful system for studying mitochondrial biology.

Keywords - mitochondrial heteroplasmy, doubly uniparental inheritance of mitochondria (DUI), *Ruditapes philippinarum*, germline, immunohistochemistry, OXPHOS.

Introduction

In most organisms, mitochondria are inherited maternally, a process known as Strictly Maternal Inheritance (SMI). Under SMI, the entire mitochondrial population derives from the egg, while sperm mitochondria are prevented from entering the zygote or

eliminated by the developing embryo through different mechanisms, for example by ubiquitination and degradation with proteases, or in lysosomes (Zhou et al. 2016; Punzi et al. 2018 and references therein). Moreover, each generation, between oogenesis and early embryogenesis, the mitochondrial population undergoes a drastic reduction in number, a process known as mitochondrial bottleneck (Bergstrom and Pritchard 1998; Mishra and Chan 2014). SMI and mitochondrial bottlenecks are considered to be partly responsible for homoplasmy, namely the presence of only one mitochondrial haplotype in an individual (Bergstrom and Pritchard 1998; White et al. 2008). The opposite condition—by which different mitochondrial DNA (mtDNA) variants are present in the same individual—is defined heteroplasmy, and it is mostly known to be associated with unfavorable conditions, diseases, and ageing (see for example: Lane 2011, 2012; Sharpley et al. 2012). Actually, heteroplasmy is much more common than previously thought, in both animals and plants (Kmiec et al. 2006; Woloszynska 2010), and how such genetic variation contributes to complex traits and diseases is still unclear (Dowling 2014). One of the reasons why assessing the effects of heteroplasmy is a difficult task is the large mtDNA copy number per cell/organelle: alleles do not show a phenotypic effect when present at mid-low frequency, so they drift in the mitochondrial gene pool without being subject to selection ("buffering", or "threshold effect": Rossignol et al. 2003; Ghiselli et al. 2013; Busch et al. 2014; Dowling 2014; Milani and Ghiselli 2015). Moreover, since one of the main functions of mitochondria, oxidative phosphorylation (OXPHOS), depends on mitonuclear matching (Lane 2011; Latorre-Pellicer et al. 2016), severe heteroplasmy—highly divergent haplotypes at high frequency—is likely an unfavourable, thus rare, condition. As a consequence, in most organisms, heteroplasmy represents a sort of "hidden genetic variation" that is difficult to study, and an exceptional model system could be extremely helpful.

The only natural and evolutionarily stable heteroplasmic system known in Metazoa is the Doubly Uniparental inheritance (DUI) of mitochondria, so far described in ~100 bivalve species (Gusman et al. 2016). In this system, two mitochondrial lineages are present: one transmitted through eggs (F-type) and the other transmitted through sperm (M-type). However, this is not a case of biparental (Mendelian) inheritance because F and M lineages are both transmitted uniparentally. Thus, conspecific F and M mtDNA show a remarkable nucleotide sequence divergence—ranging from 22% to 39% in mytilids and reaching 43% in unionids—corresponding to an amino acid sequence divergence of mitochondrial OXPHOS proteins above 50% (see Zouros

2013 for a review). The available data suggest that DUI derived from SMI through a modification of the mechanisms of degradation and segregation of sperm mitochondria (Breton et al. 2007; Passamonti and Ghiselli 2009; Milani et al. 2015, 2016; Punzi et al. 2018). The DUI transmission route is as follows. Sperm carries only M-type mtDNA while eggs carry only F-type mtDNA. During fertilization, the spermatozoon transfers the M-type mtDNA to the egg, so the zygote is heteroplasmic. By fertilizing eggs with sperm stained with MitoTracker Green, it was possible to observe the distribution of paternal mitochondria in early embryos of *Mytilus* (Cao et al. 2004; Obata and Komaru 2005; Cogswell et al. 2006; Kenchington et al. 2009) and *Ruditapes philippinarum* (Milani et al. 2011, 2012). Two patterns were observed: the aggregated pattern, in which sperm mitochondria stay clustered together and localize in the middle of the first cleavage furrow, and the dispersed pattern, in which sperm mitochondria are scattered across blastomeres. In *Mytilus* it was possible to associate the aggregated pattern with male embryos, so it was hypothesized that the aggregate of sperm-derived mitochondria ends up in germline precursor blastomeres in males (Cao et al. 2004). It was also proposed that the midbody—a cytoplasmic structure formed by the compression of the microtubule spindle during the first cleavage—is involved in the positioning of sperm mitochondria in the region that eventually gives rise to germ cells (Milani et al. 2011). It is still unclear how these two different patterns originate. It was suggested that sperm mitochondria in DUI species are tagged with ubiquitin—similarly to what observed in mammals (Sutovsky et al. 2000)—or with some sort of molecular tag that in male embryos is inactivated/masked by maternal factors, allowing sperm mitochondria to invade the germline (see models proposed in: Ghiselli et al. 2012; Diz et al. 2013; Milani, Ghiselli, Nuzhdin, et al. 2013; Zouros 2013; Punzi et al. 2018). Another hypothesis concerns the preferential transmission of mitochondria having high membrane potential ($\Delta\psi_m$) (Milani 2015). What happens next is even less clear.

A point that is well-established is the homoplasmy of gametes for the sex-specific mitochondrial lineage (F-type in eggs, M-type in sperm), strongly supported by the high sequence divergence that accumulates between the two lineages within the same species. Indeed, if the system were leaky or unstable, such divergence could not be reached. In *R. philippinarum*, qPCR analyses performed on mtDNA and mRNA targets (Ghiselli et al. 2011; Milani, Ghiselli, Iannello, et al. 2014) suggested that female somatic tissues are mostly homoplasmic for the F-type, while males are heteroplasmic. The extent of such somatic heteroplasmy in males depends on both tissue and species

(see Zouros 2013). Ghiselli et al. (2011) hypothesized that the establishment of homoplasmic gametes starting from a condition of heteroplasmy could happen through three checkpoints. Checkpoint #1 would be the sex-linked distribution patterns of sperm mitochondria in early embryo development, checkpoint #2 would consist in the degradation of M-type mitochondria in females, and checkpoint #3 would be a strict selection of sex-specific mtDNA lineages during gametogenesis. Checkpoint #2 was hypothesized because M-type was rarely detected in *R. philippinarum* females after 24 hours post fertilization (Ghiselli et al. 2011; Guerra et al. 2016).

So far, no study has investigated heteroplasmy at the protein level, and whether it occurs within tissues, cells, or organelles. The high sequence divergence between F- and M-type proteins in DUI species provides a unique opportunity to produce specific antibodies, immunolocalize the two forms, and assess level and extent of heteroplasmy. We characterized the expression of three mitochondrially-encoded proteins in the DUI species *R. philippinarum* in germline and somatic tissues of both sexes at different developmental stages. The target proteins were: NADH dehydrogenase 5 (ND5), cytochrome b (CYTB), and cytochrome c oxidase subunit III (COX3), belonging to different complexes of the electron transport chain (I, III, and IV, respectively). We produced and tested specific antibodies to discriminate the two forms (F- and M-type) of each of these three OXPHOS proteins. After specificity verification using Western blot, we proceeded with immunohistochemistry and *in situ* visualization of the targets with both confocal and transmission electron microscopy (TEM).

Some of our results are consistent with the predictions drawn from the data available in literature—such as homoplasmy in eggs and sperm—but we also present some unexpected findings that are going to change the current view of the mechanisms underlying DUI. Indeed, the presence of both F and M protein variants in early germ cells cannot be explained by the current DUI models, so we propose a revision. Lastly, we emphasize the potential of this unusual system for future research in the field of mitochondrial biology.

Materials and methods

Gonad anatomy and germline development

In bivalves, the gonad is a transient anatomical structure that consists of a series of connected tubules organized in sack-like structures named acini, in which germ cells

differentiate centripetally from the external border—a germinal epithelium defined "wall"—to the center (the "lumen"), where mature gametes accumulate (Milani, Ghiselli, Nuzhdin, et al. 2013; Milani et al. 2017, 2018). Acini are usually present at different stages of maturation, thus containing germ cells undergoing different phases of the differentiation process. During the maturation period, this tissue develops into a system of branching tubules connecting multiple acini, that are filled with mature gametes when the animal is ripe. The system of tubules merges into an excretory duct through which gametes are spawned; fertilisation is external and gametes are shed through the exhalant syphon (Gosling 2003).

Bivalve reproductive cycle is deeply affected by environmental and trophic conditions and involves four main stages: 1) a spent phase, that is a period of sexual rest; 2) a phase of gonad redevelopment/reconstruction; 3) a phase of gonad ripening/maturation (gametogenesis); and 4) a single or more spawning events (Gosling 2003). Due to the lack of any secondary sexual characteristics, sex in bivalves can be assessed only by visualization of a gametic smear under an optical microscope. During the sexual rest, when there are no gonads/gametes, sex identification is not possible.

In the Adriatic Sea, the spawning season of *R. philippinarum* occurs from late May to September (mostly between June and the end of August), then the animals enter the sexual rest until the following Spring. Clams, as *R. philippinarum*, are gonochoric, and gonads appear as a diffused, whitish mass closely associated to the digestive system. The specification of germ cells in bivalves takes place through a mechanism named preformation, by which germline determinants such as RNAs/proteins (e.g.: Vasa, Nanos, Piwi, Tudor), mitochondria, and mitochondrial components—the "germ plasm"— are stored in the egg and inherited by the progeny (Extavour and Akam 2003; Ghiselli et al. 2012; Milani, Ghiselli, Nuzhdin, et al. 2013; Solana 2013). Germ plasm components have been shown to be expressed in both multipotent cells and germ cells across diverse taxa, so Juliano et al. (2010) proposed the existence of a highly conserved germline multipotency program (GMP) operating in both types of cells. Spiralians show a highly conserved early development program, and studying the expression patterns of the germline gene set in several taxa, it was possible to trace the origin of gonads from the 4d mesentoblast, that gives rise to the visceral mesoderm and endodermal intestine (Fabioux et al. 2004; Henry et al. 2010; Lyons et al. 2012). In some bivalve species—including *R. philippinarum*—a strong association of the

intestinal epithelium with cells expressing Vasa was observed (Milani et al. 2017). It was then proposed that, at the beginning of the reproductive cycle, Primordial Stem Cells (PriSCs; see Solana 2013)—multipotent cells located in the intestinal epithelium—give rise to Primordial Germ Cells (PGCs) through an asymmetric cell division that produces a PriSC and a PGC. Then, PGCs migrate into the connective tissue originating Germinal Stem Cells (GSCs) that proliferate forming the gonad wall and gametogenesis begins. Finally, at the end of the reproductive period, gonads are reabsorbed and the animal enters the sexual rest period until, at the following reproductive season, the gonads are rebuilt from PriSCs associated with the intestinal epithelium and GSCs in the connective tissue (Milani et al. 2017, 2018). The scheme in Figure 1A summarizes the steps of germline development proposed for *R. philippinarum* and Figure 1B place the different germ cell types in an anatomical context.

Sampling

Specimens of *R. philippinarum* were collected from the Northern Adriatic Sea, in the river Po delta region (Sacca di Goro, approximate GPS coordinates: 44º50′06″N, 12º17′55″E). The sampling was performed at different times of the year to get clams at different stages of sexual maturity. More in detail: 1) 6 adult males and 6 adult females (shell size of 3-4 cm) were collected in May-June 2016 (ripe gonads); 2) 3 adult males and 3 adult females (shell size of 3-4 cm), and 5 juveniles (shell size ~1 cm) were collected in September 2016 (end of reproductive season); 3) 10 adult females were collected in November 2016 (approaching sexual rest); 4) 6 adults were collected in January 2016 (sexual rest). The sex of the latter specimens was unknown because of the absence of gonads, however, they were used for protocol optimization.

The sex of the adults was assessed by observation of gonadic tissue smears under an optical microscope, then pieces of the body containing mostly gonads and portions of adjacent somatic tissues (e.g.: digestive tube and connective tissue) were collected and directly processed for immunohistochemistry or stored at -80°C for Western blot (WB) analysis. In the case of juvenile clams, the entire body was collected due to their small size and absence of a developed gonad.

Design of M- and F-specific antibodies

M- and F-type mitochondrial OXPHOS sequences were downloaded from GenBank, aligned with ClustalW and compared to find highly divergent regions. We choose the proteins in which it was possible to find stretches of ~10-20 amino acids showing high sequence divergence between M and F forms, making such regions the most suitable to be used as immunogen peptides (Supplementary Fig. 1; Supplementary Table 1). Three proteins were chosen as best candidates for antibody production: ND5, CYTB, and COX3. Their sequences were sent to Davids Biotechnologie (Regensburg, Germany) where synthetic peptides were injected in rabbits for the production of the F-type antisera and in chicken for M-type antisera. Two different animals were needed for antibody production to allow the use of different secondary antibodies in order to perform the simultaneous staining of M and F targets (double staining). Supplementary Table 1 also reports the expected molecular weight and the concentration range used for each antibody in WB and immunohistochemistry protocols. The protein molecular weight expected for each OXPHOS protein was calculated using Compute pI/Mw (ExPASy) (http://web.expasy.org/compute_pi/).

Western blot

We ran WB of male and female gonad homogenates to determine the molecular weight of the protein bound by our antibodies. However, we could not establish *a priori* the presence/absence in the gonad of one or both the mitochondrial types (it was actually an issue we wanted to address), also, the samples contain portions of somatic tissues intimately wrapped around the gonad. So, the specificity for one OXPHOS protein type—a single band of the expected molecular weight—was determined by WB, instead, the sex-variant specificity was established by the immunological double staining, that localized only the sex-specific mitochondrial type in differentiated gametes.

Samples were homogenized using an Ultra Turrax T25 (Janke & Kunkel IKA-labortechnik) in RIPA buffer containing 50 mM Tris-HCl (pH 7.4), 150 mM NaCl, 1% detergent Tergitol-type NP-40 (nonyl phenoxypolyethoxylethanol), 0.25% Na-deoxycholate, 1 mM EDTA and protease inhibitors [1 mM PMSF and 1 mini tablet of protease inhibitor cocktail (Complete Mini, Roche) (1 mini tablet in 5 mL of buffer)] to limit the degradation of the sample. Then, samples were centrifuged at 7,500 xg for 10 min at 4°C. The supernatant was collected and stored at -80°C. The amount of total proteins in the homogenates was quantified with Lowry method (Lowry et al. 1951).

Proteins were separated via 8.5% and 12% Sodium Dodecyl Sulphate - PolyAcrylamide Gel Electrophoresis (SDS-PAGE) (Laemmli, 1970). Five µL of Bio-Rad Precision Plus Protein™ Dual Color Standards or Bio-Rad Prestained SDS-PAGE Standard Broad Range™ were also loaded for reference.

For immunoblotting, proteins were electrically transferred to nitrocellulose membranes (Amersham™ Hybond™ Blotting Membranes, Buckinghamshire, UK). Before the incubation with the primary antibody, to prevent non-specific protein binding, unspecific sites were blocked with 5% dried skimmed milk (Bio-Rad Laboratories, Hercules, CA, USA), 3% Bovine Serum Albumin (BSA), in Tris-Buffered Saline (20 mM Tris base; 137 mM NaCl) (pH 7.4) (TBS) with 0.1% Tween-20 (Sigma) (TBS-Tw), for 1 h 30 min at room temperature (RT), and subsequently washed for 30 min with TBS-Tw at RT.

Then the membranes were incubated with primary antibodies overnight at 4°C, then for 1 h 30 min at RT. After rinsing for 30 min with TBS-Tw, the membranes were incubated with the secondary antibody for 1 h at RT. Finally, the membranes were washed for 20 min with TBS-Tw and 10 with TBS.

The washed membranes were treated with ECL Western Blotting Detection Reagents (GE Healthcare) and exposed to Hyperfilm ECL (GE Healthcare). To verify antibody specificity, the synthetic peptides were added to the primary antibody solution at a 10X concentration before the incubation. This step was performed in order to chelate by competition every antigenic site of the primary antibody. In this way it is kept from binding its protein target and the specific bands is strongly attenuated.

Immunohistochemistry

Immunohistochemistry was performed to localize the antibody reaction in somatic tissues and gonads of *R. philippinarum* males and females.

A piece of the body (visceral mass) containing all the tissues of interest (intestine, connective and gonadic tissue) was excised and fixed in a solution of 3.7% paraformaldehyde, 0.1% or 0.25% (depending on sample size) glutaraldehyde in PIPES buffer 2X (piperazine-N,N′-bis(2-ethanesulfonic acid)) (160 mM K Pipes, 2 mM $MgCl_2$, 10 mM EGTA, 0.4% Triton X-100) (pH 7) for 3 h-3 h 30 min (depending on sample size) at RT. The samples were washed in Phosphate Buffered Saline (PBS) (128 mM NaCl, 2 mM KCl, 8 mM Na_2HPO_4, 2 mM KH_2PO_4) (pH 7.2) every 10-15 min for 1 h. Then samples were embedded in 7% agar and sectioned (100-200 µm thickness). The sections were post-fixed with increasing concentrations of methanol

(50–100%) and rehydrated in PBS or TBS (10 mM Tris–HCl, 155 mM NaCl) (pH 7.4) for 1 h.

Unreacted aldehydes were reduced with 70 mM sodium borohydride ($NaBH_4$) in TBS (pH 7.4) for 1 h 30 min at room temperature, followed by several washes in TBS with 0.1% Triton X-100 (TBS-Tx 0.1%) for about 2 h.

Antigens and epitopes were retrieved with 0.01% Pronase E (Merck) in PBS for 18 min at RT. Sections were rapidly washed with PBS in order to stop digestion, the last wash was with TBS-Tx 0.1%. The samples were permeabilized adding TBS-Tx 1% (pH 7.4) and left at 4°C overnight.

Non-specific protein-binding sites were blocked with a preincubation buffer; i) for anti-Rph M antibodies: 10% Normal Goat Serum (NGS) and 1% BSA in TBS-Tx 0.1% (pH 7.4) for 1 h 30 min, and ii) for anti-Rph F antibodies: 10% Normal Donkey Serum (NDS) and 1% BSA in TBS-Tx 0.1% (pH 7.4) for 1 h 30 min.

Primary antibodies were diluted with 3% BSA in TBS-Tx 0.1% (pH 7.4) and section incubation was carried out for 72 h at 4°C, followed by washes with TBS-Tx 0.1% for 26 h with several changes.

The, sections were incubated in the dark with secondary antibodies for 32 h at 4°C, and subsequently washed for 24 h with several changes in TBS-Tx 0.1% (pH 7.4). The secondary antibody was: i) for anti-Rph M antibodies: DyLight 550 Goat anti-Chicken IgG (IgY) (H+L), Cross Absorbed (1:500) (ThermoFisher Scientific), and ii) for anti-Rph F antibodies: Alexa Fluor® 488-AffiniPure Donkey antiRabbit IgG (H+L) Cross Absorbed (1:400) (Jackson ImmunoResearch). Antibodies were diluted with a dilution buffer (DI) (1% NGS for antibodies M-type and 1% NDS for antibodies F-type, 1% BSA in TBS-Tx 0.1%) (pH 7.3) for 1 h 30 min.

The primary antibodies that showed the best reaction in the WB (for strength and specificity of the signal) were also used in a contemporary, double staining, in order to visualize M and F proteins on the same section.

The nuclear counterstaining was performed with 1 mM TO-PRO®-3 nuclear dye (Life Technologies, Carlsbad, USA) in PBS (pH 7.2) for about 10 min in the dark at RT, then the dye was washed in TBS-Tx 0.1% (pH 7.4) for 30 min.

All the immunostained sections were mounted in anti-fade mounting medium (2.5% 1,4-diazabicyclo[2.2.2]octane, DABCO; Sigma), 50 mM Tris (pH 8) and 90% glycerol.

Negative controls were also carried out: two controls testing secondary antibodies and a third control without any antibody. Sections were examined with a Leica TCS SL

confocal laser scanning microscope equipped with Ar/He/Ne lasers, using Leica confocal software.

Transmission electron microscopy

TEM analysis was performed to find the ultrastructural localization of the antibody staining in specific cell types and organelles.

Pieces containing gonadic tissue were excised from 3 males and 3 females and fixed in 4% paraformaldehyde and 0.5% glutaraldehyde in 0.1 M sodium cacodylate buffer (pH 7.4). After dehydrating the samples through increasing concentrations of ethanol, they were embedded into LR White Resin. The blocks were sectioned with an Ultracut Leica UC6 ultramicrotome (Leica Microsystems, Germany) using a diamond knife. Thin sections were mounted on formvar-coated nickel grids, and the grids were floated on drops of 1% BSA/0.01% Tween-20 in PBS for 1 h. This was followed by 1 h incubation with primary antibodies against *R. philippinarum* mitochondrial proteins. As primary antibodies, those showing the best performance in the previous analyses (WB and immunohistochemistry at confocal microscopy) were used (anti-ND5_F, anti-CYTB_M, anti-COX3_M, anti-COX3_F antibodies; Supplementary Table 1 for details). All of them were diluted 1:200 with PBS-0.05% Tween-20 (PBS-0.05% Tw). Next, sections were washed in PBS-0.05% Tw and incubated for 2 h at room temperature with a PBST solution containing a mixture of secondary antibody (1:50): 12-nm colloidal gold-conjugated goat anti-rabbit IgG antibody (111-205-144, Jackson) and 18-nm colloidal gold-conjugated goat anti-chicken IgG antibody (703-215-155, Jackson). As control, primary antibodies were omitted, and only secondary antibodies were used. Sections were washed three times in PBS-0.05% Tw, rinsed in distilled water, stained with uranyl acetate and lead citrate. Observation and imaging were performed with a Zeiss Libra 120 transmission electron microscope (Karl Zeiss Group, Germany).

Results

Immunostaining shows heteroplasmy of OXPHOS proteins at tissue, cell, and organelle level

Throughout all the experiments, the tissues analyzed were gonads with adjacent somatic tissues (gut, connective tissue, and muscle tissue), and both females and males were observed at different stages of gametogenesis.

The bands obtained with WB had a molecular weight comparable to the predicted protein weight, except in the case of F-type ND5 that resulted lighter than expected (Fig. 2; Supplementary Table 1). This discrepancy can be either due to a wrong annotation of the gene, or to post-transcriptional/translational editing of the nd5 sequence. In any case, the ND5 protein seems to have a different weight in the two sexes.

At the confocal microscopy, the staining was localized in spots of ~ 500 nm, compatible with the dimension of mitochondria (e.g.: Fig. 3I,J).

Antibody specificity for F- and M-type mitochondrial variants was supported by the homoplasmy detected in differentiated gametes—oocytes positive for the F-type staining, spermatozoa for the M-type staining—observed at TEM with simultaneous staining with F- and M-type antibodies.

In control sections with only secondary antibody treatment, no staining was observed (Supplementary Fig. 2).

F-type protein variants

In female samples, anti-F antibody staining was visible in somatic cells of the connective tissue and of the intestinal epithelium (batiprismatic cells) (Fig. 3O,P) and in muscle cells (Fig. 3Q). Also, anti-F antibody stained the cytoplasm of undifferentiated/early germ cells around developing oocytes (Fig. 3E,F insets) and the cytoplasm of oocytes at different phases of maturation (Fig. 3E,F).

In male samples, anti-F antibody staining was detected in somatic tissues (batiprismatic cells Fig. 3K-N, connective tissue Fig. 3K,L, and muscle cells Fig. 3J).

A very strong staining was observed in cells with a small nucleus, located in the basal part of the intestinal epithelium, that can be identified as PriSCs (Fig. 3K-M). Differentiating male germ cells (spermatocyte and spermatids) showed anti-F staining, but spermatozoa did not (Fig. 3B,C).

M-type protein variants

In male samples, anti-M staining was observed in batiprismatic cells, in the connective tissue and muscle cells (Fig. 3G-I). Anti-M staining was observed in male early germ cells, according to morphology and localization (Fig. 3A,C). Anti-M antibody staining was present in PriSCs located at the basal side of the gut epithelium, close to the

connective tissue (Fig. 3G), in PGCs/GSCs inside the connective tissue (Fig. 3H and inset).

In female samples, no significant anti-M staining was observed neither in oocytes (Fig. 3D) nor in somatic cells of the gut and connective tissue (Fig. 3P). Instead, the staining was observed in cells with a round nucleus localized around acini, these cells resembling undifferentiated/early germ cells (Fig. 3E,F).

Summarizing, undifferentiated germ cells were positive for both anti-F and anti-M antibodies both in females (Fig. 3E,F and inset) and males (Fig. 3C).

Double staining with anti-F and anti-M antibodies

The co-expression of the two variants was also verified with the contemporary staining with anti-F and anti-M antibody. The double staining was observed in PriSCs located at the basal pole of the intestine (Fig. 3K-N) and in PGCs/GSCs in the connective tissue (for example in Fig. 3H).

Immuno-transmission electron microscopy highlighted the presence of both the mitochondrial protein variants (M+F) in undifferentiated/early germ cells, while gametes were homoplasmic (oocytes for the F type, spermatozoa for the M type) (Figs. 4, 5).

Discussion

Level and extent of heteroplasmy

In this work we obtained lineage-specific (F-type-specific and M-type-specific) antibodies for three mitochondrial proteins of the OXPHOS pathway (ND5, CYTB, and COX3), and studied their localization by confocal and transmission electron microscopy in female and male tissues of the Manila clam (*R. philippinarum*) at different developmental stages.

In females, both variants were detected in PriSCs, in undifferentiated germ cells, and in early oocytes, but no M-type protein was observed in mature eggs and in the soma (Fig. 3). In males, both labelling were visible in PriSCs, undifferentiated germ cells, and in somatic tissues, but no F-type labelling was observed in spermatozoa (Fig. 3) (a summary of antibody localization in Supplementary Table 2; a scheme of the staining in Supplementary Fig. 3). Moreover, heteroplasmy was observed at the organelle level,

namely both F- and M-type protein variants were present in the same mitochondrion (Figs. 4, 5).

The expression pattern of F-type mitochondrial proteins in germline and somatic tissues of females is coherent with the results of qPCR analyses on mtDNA (Ghiselli et al. 2011). According to previous works, DUI females are generally homoplasmic for the F-type mtDNA (Ghiselli et al. 2011; Milani et al. 2012; Zouros 2013; Guerra et al. 2016), so the consistent M-type staining in the undifferentiated germline lineage was unexpected. However, we got support to antibody specificity for a single variant by the immunological double staining on mature gamete ultrastructures (Figs. 4, 5), that showed only the sex-specific mitochondrial type, in accordance to the mtDNA gamete homoplasmy resulted from qPCR (Ghiselli et al. 2011).

As reported in the literature, *R. philippinarum* males are heteroplasmic in somatic tissues, but homoplasmic for the M-type in gametes (Ghiselli et al. 2011; Milani, Ghiselli, Iannello, et al. 2014). In male samples, as expected, M-type antibodies stained both somatic tissues and germ cells (Fig. 3-5). F-type antibodies in males confirmed the mitochondrial heteroplasmy also at the protein level in somatic tissues, since F-type mitochondria were labeled in the intestinal epithelium, in the connective tissue, and in muscle cells (Fig. 3).

Implications for the DUI system

The data obtained in this work allow, for the first time, to visualize the distribution of F- and M-type OXPHOS subunits, and provide new information about the DUI system, including some unexpected finding. The most surprising result is the presence of both F- and M-type proteins in PriSCs, PGCs, GSCs, and oogonia or spermatogonia, in males and females. This means that also females are heteroplasmic—even if to a lesser extent with respect to males—and that some of the hypotheses that have been made about the dynamics of the two mitochondrial lineages need to be revised. The checkpoint #1, which corresponds to the lineage-specific distribution pattern of M-type mitochondria in early embryos—dispersed in females, aggregated in males—was proposed to be the mechanism by which sperm mitochondria reach the germline in males, but not in females (Ghiselli et al. 2011). The present data show that M-type mitochondria reach the germline irrespectively from the sex of the individual, so the hypothesized function of the two distribution patterns needs to be reconsidered. A second checkpoint consisting in the selective degradation of M-type mitochondria in

females (analogously to what happens in some SMI organisms) was also proposed. There was already evidence that checkpoint #2 could be sometimes ineffective, given the finding of M-type-positive female somatic tissues (Ghiselli et al. 2011), but in the light of the results presented here, we think that its actual existence should be reconsidered, as well. Indeed, given the consistent finding of M-type proteins in female PriSCs and undifferentiated germ cells, either this checkpoint does not exist at all—meaning that there is no degradation mechanism of sperm mitochondria in this species—or its action, when successful, is limited to female somatic cells. Instead, these new results strongly support the existence of checkpoint #3, that is the segregation of sex-specific mtDNA lineages in mature gametes (F-type in eggs, M-type in sperm). This checkpoint was originally defined as "a filter for germline mitochondria, and it may operate when PGCs establish themselves (i.e., whenever PGCs do separate from somatic cells)" (Ghiselli et al. 2011), but such definition needs to be updated, because here we show that such filter is operating at a later stage, most likely during meiosis. In this light, the mechanism of segregation distortion in favor of F mitochondria in eggs and M mitochondria in sperm can be viewed as a case of meiotic drive. How is such distortion achieved?

Since the dawn of DUI research, one of the primary goals was to identify the genetic elements involved in the deviation from SMI. Bivalve genomics resources are still scarce and/or low-quality, but a fair amount of complete mitochondrial genomes of DUI species has been available for a while; for this reason, research has been focusing on finding such elements in the F- and M-mtDNAs. MtDNAs of bivalves are generally rich in unassigned regions (Ghiselli et al. 2013), namely regions of the genome that cannot be annotated. Several works that analyzed such regions in different species reported the presence of ORFans (open reading frames having no detectable sequence similarity to other known proteins; see Fischer and Eisenberg 1999), that became candidates for having a role in the DUI system (Breton et al. 2009; Breton, Ghiselli, et al. 2011; Breton, Stewart, et al. 2011; Ghiselli et al. 2013; Milani, Ghiselli, Guerra, et al. 2013; Milani, Ghiselli, Maurizii, et al. 2014; 2015, 2016; Mitchell et al. 2016). In a study on *R. philippinarum*, Milani et al. (2015) observed that a M-type-specific ORFan named RPHM21, is expressed only in a subset of PriSCs, while it is present in all the spermatozoa. The expression pattern observed for RPHM21 is consistent with that reported here for three M-type OXPHOS subunits: in males, M-type proteins are either absent or present together with F-type variants in cells expressing a germline

multipotency program (Juliano et al. 2010), but they become the only variant present in post-meiotic cells. A working hypothesis posits that, during spermatogenesis, germ cells carrying the M-type mtDNA and expressing RPHM21 gain some sort of advantage over the germ cells not expressing it. In particular, a faster proliferation of RPHM21-positive germ cells was proposed as a potential underlying mechanism, but another possibility that we would like to suggest here is that of RPHM21 being a "killer meiotic driver", namely a selfish genetic element that can spread through a population by actively destroying competitors (Bravo Núñez et al. 2018).

A mechanism of meiotic drive involving killer ORFs produced by mitochondria or chloroplasts is well known in numerous species of gynodioecious plants: it is the Cytoplasmic Male Sterility (CMS; reviewed in Chase 2007). In species with CMS, novel mitochondrial ORFs produce chimeric proteins that cause male sterility. In rice, for example, ORF79 protein—which is toxic when expressed in *Escherichia coli*—accumulates in microspores (spores that will develop into male gametophytes). Two nuclear genes can restore male fertility by blocking ORF79 via endonucleolytic cleavage or degradation (Wang et al. 2006).

In the future, it would be interesting to look for similarities between the DUI and the CMS systems—if any—to track down the molecular mechanisms behind DUI. So far only two bivalve mitochondrial ORFans have been analyzed more in depth, and each found to actually produce a protein: a F-type specific ORFan in the freshwater mussel *Venustaconcha ellipsiformis* (Breton, Stewart, et al. 2011), and the above-mentioned M-type specific RPHM21 in *R. philippinarum* (Milani, Ghiselli, Maurizii, et al. 2014). Comparative *in silico* analyses found high sequence divergence across bivalve ORFans, but similar structural features (Milani, Ghiselli, Guerra, et al. 2013; Mitchell et al. 2016), something that might indicate a shared function. Much more work is needed to understand the function of these novel mitochondrial proteins and to elucidate the molecular mechanisms of DUI, but we can advance a new working hypothesis taking into account the findings reported here.

A revised model for DUI

Gametes are homoplasmic for the respective sex-specific mitochondrial lineage (F-type in eggs, M-type in sperm), and upon fertilization the embryo is heteroplasmic. According to the previous model of DUI, such heteroplasmic condition persists only in males, where the cluster of sperm mitochondria reaches the 4d blastomere and then

the gonad (checkpoint #1, aggregated pattern). In females, sperm mitochondria are dispersed (checkpoint #1, dispersed pattern) and degraded (checkpoint #2). The observations reported here show that M-type mitochondria can reach the cells that inherit the germ plasm in both males and females. How? In oocytes of several model animals (see for example: Wilding et al. 2001; Cox and Spradling 2003; Zhang et al. 2008; Zhou et al. 2010; Bilinski et al. 2017), it was reported that mitochondria showing a high $\Delta\psi_m$ are preferentially imported into the Balbiani Body, a cytoplasmic structure that includes the germ plasm (Kloc et al. 2004). Accordingly, Milani (2015) proposed that sperm mitochondria—if not degraded or excluded from the embryo—can reach the germ plasm because of their higher $\Delta\psi_m$, a mechanism that might explain why M-type mitochondria invade the germline in DUI organisms.

A point that is difficult to explain is the different occurrence and extent of heteroplasmy between female and male somatic tissues. Females with heteroplasmic soma have been reported, but they seem to be much rarer than males, for which somatic heteroplasmy is instead a common condition—with M-type being often dominant in some male tissues of *R. philippinarum* (Ghiselli et al. 2011). The available data do not allow us to formulate clear hypotheses, however, it is possible that the different pattern of mitochondrial segregation plays a role in this.

In contrast, we have now fairly more information about what happens next in the germline: in both the sexes, the switch between heteroplasmy and homoplasmy occurs during meiosis, and this seems to be the only existing—or the only effective—checkpoint (checkpoint #3). DUI then appears to be based on a process of meiotic drive that happens either in both oogenesis and spermatogenesis, or only in spermatogenesis. In the first case, we would have two drivers—the F-type in oogenesis and the M-type in spermatogenesis—while in the second case the driver would be the M-type, and its spread would be successful in spermatogenesis but not in oogenesis.

There are several types of meiotic drive, encompassing a broad range of mechanisms that can act at different stages of meiosis (Lindholm et al. 2016). Bivalve molluscs such as *R. philippinarum* and *Mytilus* produce the so-called class II oocytes, in which meiosis is arrested in prophase I, reinitiated, and secondarily arrested in metaphase I before the extrusion of the first polar body (Colas and Dubé 1998); meiosis is reactivated and completed after fertilization. Mitochondria of late oocytes in female acini showed only the F-type labelling, so if the drive mechanism operates in both the sexes (two-drivers

hypothesis) and at the same stage of gametogenesis, it is probably acting in prophase I. Further possibilities are: *i)* the drive occurs in both sexes but with different mechanisms at different stages of meiosis; *ii)* the drive occurs only in males (one-driver hypothesis) but the different dynamics of meiosis during oogenesis (e.g.: meiotic arrest, asymmetry) prevent the M-type-linked driver from being successful in females.

Mitochondria, germline, and sex

There is a tight interconnection between mitochondria and germ plasm, and mitochondria have been shown to be actively involved in germline formation, especially through the interaction with other elements of the Balbiani body. Not only the Balbiani body has been proposed as the structure responsible for the selection of germline mitochondria, but there is evidence of a contribution of mitochondrial material (e.g.: ribosomes and proteins) to the germ plasm (Kobayashi et al. 1993; Reunov et al. 2000, 2018; Amikura et al. 2001, 2005; Isaeva 2001; Reunov 2004; Ninomiya and Ichinose 2007; Bilinski et al. 2017). Reunov et al. (2019) investigated the activity of germ plasm and associated structures during the mitosis-to-meiosis shift in *R. philippinarum*, and observed an interplay between germ plasm and mitochondrial material during the triggering of meiosis onset in both sexes. More in detail, the Authors found that the shift from mitosis to meiosis in both females and males involves a phase in which a VASA-positive substance enters the mitochondria that are disassembled and release their content in the germ plasm. We think that the drive process is occurring at this stage (prezygotene-pachytene) or shortly after. During this phase, mitochondrial elements (ribosomes, F- and M-specific factors such as RPHM21, other ORFans, RNAs, etc.; Milani et al. 2016; Pozzi et al. 2017) could interact among each other, with the germ plasm, and with the nucleus, contributing to germline development and influencing the mitochondrial inheritance process.

Overall, there is an increasingly large portion of the evolutionary literature advocating a role for mitochondria in the origin of sex (Lane and Martin 2010; Hadjivasiliou et al. 2013; Radzvilavicius and Blackstone 2015; Garg and Martin 2016), and the strong interactions between mitochondria and germ plasm observed in a wide range of organisms is clearly consistent with such view. Given the evident modifications of mitochondria around germ plasm and nucleus in proximity of the mitosis-to-meiosis transition, and the clear contribution of mitochondrially-derived material in germline development, it is tempting to speculate that broken mitochondrial membranes and

mitochondrial content may be necessary to activate meiosis. Taking the speculation even further, we might hypothesize that mitochondria, in some conditions, can trigger either spermatogenesis or oogenesis, thus being responsible of sexual differentiation. This might seem an outrageous conjecture, but it is worth noting that some α-proteobacteria—the closest living relatives of mitochondria—can distort the sex ratio of their host.

Evolutionary significance of DUI

The biological function, if any, and the evolutionary significance of DUI are still unknown: it is not clear whether the tight linkage between the type of mtDNA inherited and the sex of the individual transmitting it is coincidental or causal. In the first case, sex and mitochondrial type would be just associated, meaning that the driver(s) evolved the ability to spread in a specific meiotic environment (spermatogenesis/oogenesis), but no specific functions or adaptive roles at the level of the whole individual are responsible for the origin of the system. After its origin, DUI might have been maintained for such an extensive evolutionary time (hundreds of millions of years) because of some advantageous "side-effects", like as having both mtDNAs under selection; indeed, DUI is the only known biological system in which a mtDNA can be under selection for male functions (Ghiselli et al. 2013; Milani and Ghiselli 2015; Milani et al. 2016; Skibinski et al. 2017). In the second case, mitochondrial type could be causally linked to sex, namely mitochondria could be involved in the process of sexual differentiation. If we consider that there is no sexual dimorphism in clams and that the difference between females and males lies in the type of gametogenesis carried out by the animal, the above-hypothesized manipulation of meiosis by a mitochondrial driver would actually become a sex-differentiation system. Needless to say, this is an intriguing, yet speculative, possibility.

Broader implications and future perspectives

After 25 years since its discovery, and despite 115+ papers published by ~20 different research groups around the world, DUI is still mostly overlooked, or considered just a curious feature limited to a few species, a transient phenomenon, or both. We argue that this could not be farther from the truth: the DUI system is evolutionarily stable (e.g.: it dates back 200+ million years in Unionids; see Breton, Ghiselli, et al. 2011) and its distribution across bivalve species is consistent (100+ species reported so far). Most

importantly, it represents a precious system to study several aspects of mitochondrial biology and evolution, thanks to its unique features. Of course, the condition of natural heteroplasmy with highly divergent mtDNAs opens up the possibility for performing observations and experiments that would not be possible in other organisms, or that would require very expensive manipulation techniques and/or breeding programs.

In the last few years, mitonuclear interactions have gained a great deal of attention in the field of life science, and the central role of mitochondria in almost every aspect of eukaryote life has been increasingly acknowledged. The DUI system can be extremely helpful in studying mitonuclear interactions and mitonuclear coevolution, and one of the first questions that come to mind is: “How can the nuclear genome deal with two very different mtDNAs?”. We still do not know. Sex-specific alleles/paralogs/splice forms interacting each with the corresponding mtDNA? Protein structure robustness (i.e.: high divergence at the mtDNA level but very similar protein structures)? Relaxed mitonuclear match due to lower metabolic needs and/or physiological adaptations to hypoxia/anoxia? Actually, since bivalve molluscs have anaerobically functioning mitochondria—namely facultatively anaerobic mitochondria (see class 2 mitochondria in Müller et al. 2012)—and because of their adaptations to infaunal and intertidal environment (Sokolova 2018), it is possible that their tolerance to mitochondrial heteroplasmy is much higher in respect with other animals. Another interesting and difficult topic that DUI could help unveiling is fission-fusion dynamics, again thanks to natural heteroplasmy with highly divergent variants.

A research area that could benefit even more from exploiting DUI as model system is that of germline development. The features discussed in this work—interactions of mitochondria with germ plasm and Balbiani body—are evidently widespread across a large range of biodiversity, and this means that the study of DUI animals can help to draw more general conclusions by means of comparative approaches.

Author contributions

L.M. conceived the study.

M.G.M., H.A., C.C., A.P., A.R., Y.A., S.B., and L.M. performed the experiments.

F.G., M.G.M., A.R., and L.M. analyzed the data.

F.G., M.G.M., and L.M. wrote the manuscript.

H.A., C.C, M.P., and V.F. revised the manuscript.

All authors approved the final version of the manuscript.

Acknowledgements

We gratefully thank Justin Havird and Geoffrey Hill for organizing the Symposium "Beyond the powerhouse: integrating mitonuclear evolution, physiology, and theory in comparative biology", and all the participants for their interesting and exciting contributions. We also thank two anonymous Reviewers for their valuable contribution to the improvement of the manuscript.

Funding

This work was supported by the Italian Ministry of Education, University and Research (MIUR) SIR Programme grant No. RBSI14G0P5 funded to L.M., MIUR FIR2013 Programme grant No. RBFR13T97A funded to F.G., "Ricerca Fondamentale Orientata" (RFO) funding from the University of Bologna to F.G., M.G.M., L.M., and the Canziani bequest funded to F.G. and M.P.

Travel and support funds for attending the 2019 meeting of the Society for Integrative and Comparative Biology came from the National Science Foundation (IOS-1839203), the Company of Biologists (EA1694), The Crustacean Society, and the Divisions of Comparative Physiology and Biochemistry, Invertebrate Zoology, and Phylogenetics and Comparative Biology.

Figure captions

Fig. 1. Germline formation in *R. philippinarum*. A: The scheme represents the suggested process of germline differentiation based on the results previously obtained on the species (Milani et al. 2017, 2018). Primordial Stem Cells (PriSCs); Primordial Germ Cells (PGCs); Germinal Stem Cells (GSCs). **B:** Histological view of a female sample with indication about the localization of germ cell types. Hematoxylin and eosin staining following the method in Bettini et al. (2012).

Fig. 2. Western blot. Western Blot of female and male gonadic extracts using anti-F and anti-M-type antibodies, respectively. Numbers indicate the molecular weight in kilodaltons of the adjacent band. Molecular weight standard lanes (St). The standards used are: Bio-Rad Precision Plus Protein™ Dual Color Standards (with a band of 75 kDa, pink) or Bio-Rad Prestained SDS-PAGE Standard Broad Range™. The bands

detected with the three Ab-F **(A)** and the three Ab-M **(B)** are indicated by an arrowhead. A clear reduction of these F and M bands is visible in WB in which the anti-F-type **(C)** and the anti-M-type **(D)** antibodies are utilized after incubation with the corresponding synthetic peptide at a concentration of at least 10X compared to that of the primary antibodies. **E,F)** Example of WB optimization obtained for a couple of antibodies used in the double staining. F-ND5 lane, F-type antibody on female homogenate (RIPA buffer Ab1 1: 5,000). M-CYTB lane, M-type antibody on male homogenate (RIPA buffer; Ab1 1: 500 in 1% dried skimmed milk). Other details for antibody production and usage are reported in Suppl. Fig. 1 and Suppl. Table 1.

Fig. 3. Immunolocalization of M- and F-type mitochondrial proteins in germ cells (A-F) and in somatic tissues (G-Q) of *R. philippinarum* at confocal microscope. Colors: anti-M-type, red; anti-F-type, yellow; TO-PRO®-3 nuclear dye, green. Abbreviations in alphabetical order: batiprismatic cells of the intestinal epithelium, bc; basal membrane, bm; cytoplasm, c; connective tissue cells, ct; intestinal lumen, il; muscle cells, mc; nucleus, n; spermatozoa, s; spermatocytes, sc; spermatogonia, sg. PriSCs indicated by arrowhead. Differentiating germ cells show in the cytoplasm mitochondrial-size spots stained with one or the other type of antibody. **A-C: Male germ cells. A:** Anti-M antibody staining. In sc and sg. **B:** Anti-F antibody. In male germ cells. **C:** Anti-M/-F antibody double staining. In male germ cells. **D-F: Female germ cells. D:** Anti-M antibody staining. No staining is observed in late oocytes (one is circled in dotted line; chromosomes are visible at the periphery of n). **E, F:** Anti-M/-F antibody double staining. Only F-type mitochondria are visible in late oocytes. Both anti-M and anti-F stained spots are present in early germ cells at the periphery of the acini (early germ cells magnified in the insets). **G-N: Male soma. G-I:** Anti-M antibody staining. **G:** In ct, in bc (top right inset) and in putative PriSCs (lower left inset). **H:** Low labelling in ct and strong labelling in PriSCs (inset). **I:** In some males, mc are strongly labelled with M-type antibody. **J:** Anti-F antibody. In other males, mc are F-type antibody labelled. **K-N:** Anti-M/-F antibody double staining. **K, L:** F-type mitochondria in bc; low F-type staining in ct. At higher magnification, a clear double staining is visible in PriSCs located close to bm (insets). **M:** Two PriSCs (circled) near bm with a prevalence of yellow (on the left) or red spots (on the right). **N:** A prevalent F-type staining is visible in bc, while some PriSCs (one shown) show a prevalence of M-type staining. **O-Q: Female somatic tissues. O:** Anti-F antibody. Present in ct and bc. **P,**

Q: Anti-M/-F antibody double staining. **P:** Only F-type mitochondria in ct and bc. **Q:** Only F-type mitochondria in mc. See also Suppl. Figs. 2,3 and Suppl. Table 2.

Fig. 4. Female germline of *R. philippinarum* with double immunostaining at TEM. **A,B** and **E,F:** anti-F_ND5 (12 nm) and anti-M_CYTB (18 nm). **C,D** and **G,H:** anti-F_COX3 (12 nm) and anti-M_COX3 (18 nm). Early germ cells (**A,C**) have mitochondria with both types of labelling (F- and M-type); **B,D**: magnification of the mitochondria in the white boxes in **A** and **C**, respectively (12 nm and 18 nm dots, arrow and arrowhead, respectively). Late oocytes (portions in **E,G**) have mitochondria with only F-type labelling (12 nm) (**F,H**: magnification of the mitochondria in the white boxes in **E** and **G**, respectively). Nuclei, n. Scale bars: left column 2 μm; right column 0.2 μm.

Fig. 5. Male germline of *R. philippinarum* with double immunostaining at TEM. **A,B** and **F:** anti-F_ND5 (12 nm) and anti-M_CYTB (18 nm). **C,D** and **G:** anti-F_COX3 (12 nm) and anti-M_COX3 (18 nm). Early germ cells (**A,C**) have mitochondria with both types of labelling (F- and M-type); **B,D**: magnification of the mitochondria in the white boxes in **A** and **C**, respectively) (12 nm and 18 nm dots, arrow and arrowhead, respectively). Spermatozoa (**E)** have mitochondria (m) with only M-type labelling (18 nm), magnified in (**F,G**). Nuclei, n. Scale bars: left column 2 μm; right column 0.2 μm.

Supplementary Fig. 1. Alignments of F- and M-type of mitochondrial proteins (ND5, CYTB and COX3)

Supplementary Fig. 2. Control sections for the immunological analyses in which the primary antibodies were omitted (-Ab1)

Supplementary Fig. 3. Schematic representation of mitochondrial segregation during germline differentiation in the DUI species *R. philippinarum*

Supplementary Table 1. Characteristics of primary antibodies and OXPHOS proteins

Supplementary Table 2. Summary of the localization of anti-OXPHOS staining in female and male tissues

References

Amikura R, Kashikawa M, Nakamura A, Kobayashi S. 2001. Presence of mitochondria-type ribosomes outside mitochondria in germ plasm of *Drosophila* embryos. Proc Natl Acad Sci U S A 98:9133–38.

Amikura R, Sato K, Kobayashi S. 2005. Role of mitochondrial ribosome-dependent translation in germline formation in *Drosophila* embryos. Mech Dev 122:1087–93.

Bergstrom CT, Pritchard J. 1998. Germline bottlenecks and the evolutionary maintenance of mitochondrial genomes. Genetics 149:2135–46.

Bettini S, Lazzari M, Franceschini V. 2012. Quantitative analysis of crypt cell population during postnatal development of the olfactory organ of the guppy, *Poecilia reticulata* (Teleostei, Poecilidae), from birth to sexual maturity. J Exp Biol 215:2711–15.

Bilinski SM, Kloc M, Tworzydlo W. 2017. Selection of mitochondria in female germline cells: is Balbiani body implicated in this process? J Assist Reprod Genet 34:1405–12.

Bravo Núñez MA, Nuckolls NL, Zanders SE. 2018. Genetic Villains: Killer Meiotic Drivers. Trends Genet 34:424–33.

Breton S, Beaupré HD, Stewart DT, Hoeh WR, Blier PU. 2007. The unusual system of doubly uniparental inheritance of mtDNA: isn't one enough? Trends Genet 23:465–74.

Breton S, Beaupré HD, Stewart DT, Piontkivska H, Karmakar M, Bogan AE, Blier PU, Hoeh WR. 2009. Comparative mitochondrial genomics of freshwater mussels (Bivalvia: Unionoida) with doubly uniparental inheritance of mtDNA: gender-specific open reading frames and putative origins of replication. Genetics 183:1575–89.

Breton S, Ghiselli F, Passamonti M, Milani L, Stewart DT, Hoeh WR. 2011. Evidence for a fourteenth mtDNA-encoded protein in the female-transmitted mtDNA of marine Mussels (Bivalvia: Mytilidae). PLoS One 6:e19365.

Breton S, Stewart DT, Shepardson S, Trdan RJ, Bogan AE, Chapman EG, Ruminas AJ, Piontkivska H, Hoeh WR. 2011. Novel protein genes in animal mtDNA: a new sex determination system in freshwater mussels (Bivalvia: Unionoida)? Mol

Biol Evol 28:1645–59.

Busch KB, Kowald A, Spelbrink JN. 2014. Quality matters: how does mitochondrial network dynamics and quality control impact on mtDNA integrity? Philos Trans R Soc Lond B Biol Sci 369:20130442.

Cao L, Kenchington E, Zouros E. 2004. Differential segregation patterns of sperm mitochondria in embryos of the blue mussel (*Mytilus edulis*). Genetics 166:883–94.

Chase CD. 2007. Cytoplasmic male sterility: a window to the world of plant mitochondrial-nuclear interactions. Trends Genet 23:81–90.

Cogswell AT, Kenchington ELR, Zouros E. 2006. Segregation of sperm mitochondria in two- and four-cell embryos of the blue mussel *Mytilus edulis*: Implications for the mechanism of doubly uniparental inheritance of mitochondrial DNA. Genome 49:799–807.

Colas P, Dubé F. 1998. Meiotic maturation in mollusc oocytes. Semin Cell Dev Biol 9:539–48.

Cox RT, Spradling AC. 2003. A Balbiani body and the fusome mediate mitochondrial inheritance during *Drosophila* oogenesis. Development 130:1579–90.

Diz AP, Dudley E, Cogswell A, MacDonald BW, Kenchington ELR, Zouros E, Skibinski DOF. 2013. Proteomic analysis of eggs from *Mytilus edulis* females differing in mitochondrial DNA transmission mode. Mol Cell Proteomics 12:3068–80.

Dowling DK. 2014. Evolutionary perspectives on the links between mitochondrial genotype and disease phenotype. Biochim Biophys Acta 1840:1393–1403.

Extavour CG, Akam M. 2003. Mechanisms of germ cell specification across the metazoans: epigenesis and preformation. Development 130:5869–84.

Fabioux C, Pouvreau S, Le Roux F, Huvet A. 2004. The oyster vasa-like gene: a specific marker of the germline in *Crassostrea gigas*. Biochem Biophys Res Commun 315:897–904.

Fischer D, Eisenberg D. 1999. Finding families for genomic ORFans. Bioinformatics 15:759–62.

Garg SG, Martin WF. 2016. Mitochondria, the Cell Cycle, and the Origin of Sex via a Syncytial Eukaryote Common Ancestor. Genome Biol Evol 8:1950–70.

Ghiselli F, Milani L, Chang PL, Hedgecock D, Davis JP, Nuzhdin SV, Passamonti M. 2012. De Novo assembly of the Manila clam *Ruditapes philippinarum*

transcriptome provides new insights into expression bias, mitochondrial doubly uniparental inheritance and sex determination. Mol Biol Evol 29:771–86.

Ghiselli F, Milani L, Guerra D, Chang PL, Breton S, Nuzhdin SV, Passamonti M. 2013. Structure, transcription, and variability of metazoan mitochondrial genome: perspectives from an unusual mitochondrial inheritance system. Genome Biol Evol 5:1535–54.

Ghiselli F, Milani L, Passamonti M. 2011. Strict sex-specific mtDNA segregation in the germ line of the DUI species *Venerupis philippinarum* (Bivalvia: Veneridae). Mol Biol Evol 28:949–61.

Gosling EM. 2003. Bivalve molluscs Wiley Online Library.

Guerra D, Ghiselli F, Milani L, Breton S, Passamonti M. 2016. Early replication dynamics of sex-linked mitochondrial DNAs in the doubly uniparental inheritance species *Ruditapes philippinarum* (Bivalvia Veneridae). Heredity 116:324–32.

Gusman A, Lecomte S, Stewart DT, Passamonti M, Breton S. 2016. Pursuing the quest for better understanding the taxonomic distribution of the system of doubly uniparental inheritance of mtDNA. PeerJ 4:e2760.

Hadjivasiliou Z, Lane N, Seymour RMM, Pomiankowski A. 2013. Dynamics of mitochondrial inheritance in the evolution of binary mating types and two sexes. Proceedings of the Royal Society B: Biological Sciences 280:20131920.

Henry JJ, Collin R, Perry KJ. 2010. The slipper snail, *Crepidula*: an emerging lophotrochozoan model system. Biol Bull 218:211–29.

Isaeva RA V. 2001. Germ Plasm and Germ-line Cell Determination: The Role of Mitochondria. Dev Biol 27:7.

Juliano CE, Swartz SZ, Wessel GM. 2010. A conserved germline multipotency program. Development 137:4113–26.

Kenchington EL, Hamilton L, Cogswell A, Zouros E. 2009. Paternal mtDNA and maleness are co-inherited but not causally linked in mytilid mussels. PLoS One 4:e6976.

Kloc M, Bilinski S, Etkin LD. 2004. The Balbiani body and germ cell determinants: 150 years later. Curr Top Dev Biol 59:1–36.

Kmiec B, Woloszynska M, Janska H. 2006. Heteroplasmy as a common state of mitochondrial genetic information in plants and animals. Curr Genet 50:149–59.

Kobayashi S, Amikura R, Okada M. 1993. Presence of mitochondrial large ribosomal RNA outside mitochondria in germ plasm of *Drosophila melanogaster*. Science

260:1521–24.

Lane N. 2011. Mitonuclear match: optimizing fitness and fertility over generations drives ageing within generations. Bioessays 33:860–69.

Lane N. 2012. The problem with mixing mitochondria. Cell 151:246–48.

Lane N, Martin W. 2010. The energetics of genome complexity. Nature 467:929–34.

Latorre-Pellicer A, Moreno-Loshuertos R, Lechuga-Vieco AV, Sánchez-Cabo F, Torroja C, Acín-Pérez R, Calvo E, Aix E, González-Guerra A, Logan A, Bernad-Miana ML, Romanos E, Cruz R, Cogliati S, Sobrino B, Carracedo Á, Pérez-Martos A, Fernández-Silva P, Ruíz-Cabello J, Murphy MP, Flores I, Vázquez J, Enríquez JA. 2016. Mitochondrial and nuclear DNA matching shapes metabolism and healthy ageing. Nature.

Lindholm AK, Dyer KA, Firman RC, Fishman L, Forstmeier W, Holman L, Johannesson H, Knief U, Kokko H, Larracuente AM, Manser A, Montchamp-Moreau C, Petrosyan VG, Pomiankowski A, Presgraves DC, Safronova LD, Sutter A, Unckless RL, Verspoor RL, Wedell N, Wilkinson GS, Price TAR. 2016. The Ecology and Evolutionary Dynamics of Meiotic Drive. Trends Ecol Evol.

Lowry OH, Rosebrough NJ, Farr AL, Randall RJ. 1951. Protein measurement with the Folin phenol reagent. J Biol Chem 193:265–75.

Lyons DC, Perry KJ, Lesoway MP, Henry JQ. 2012. Cleavage pattern and fate map of the mesentoblast, 4d, in the gastropod *Crepidula*: a hallmark of spiralian development. Evodevo 3:21.

Milani L. 2015. Mitochondrial membrane potential: a trait involved in organelle inheritance? Biol Lett 11.

Milani L, Ghiselli F. 2015. Mitochondrial activity in gametes and transmission of viable mtDNA. Biol Direct 10:22.

Milani L, Ghiselli F, Guerra D, Breton S, Passamonti M. 2013. A comparative analysis of mitochondrial ORFans: new clues on their origin and role in species with doubly uniparental inheritance of mitochondria. Genome Biol Evol 5:1408–34.

Milani L, Ghiselli F, Iannello M, Passamonti M. 2014. Evidence for somatic transcription of male-transmitted mitochondrial genome in the DUI species *Ruditapes philippinarum* (Bivalvia: Veneridae). Curr Genet 60:163–73.

Milani L, Ghiselli F, Maurizii MG, Nuzhdin SV, Passamonti M. 2014. Paternally transmitted mitochondria express a new gene of potential viral origin. Genome

Biol Evol 6:391–405.

Milani L, Ghiselli F, Maurizii MG, Passamonti M. 2011. Doubly uniparental inheritance of mitochondria as a model system for studying germ line formation. PLoS One 6:e28194.

Milani L, Ghiselli F, Nuzhdin SV, Passamonti M. 2013. Nuclear genes with sex bias in *Ruditapes philippinarum* (Bivalvia, veneridae): Mitochondrial inheritance and sex determination in DUI species. J Exp Zool B Mol Dev Evol 320:442–54.

Milani L, Ghiselli F, Passamonti M. 2012. Sex-linked mitochondrial behavior during early embryo development in *Ruditapes philippinarum* (Bivalvia Veneridae) a species with the Doubly Uniparental Inheritance (DUI) of mitochondria. J Exp Zool B Mol Dev Evol 318:182–89.

Milani L, Ghiselli F, Passamonti M. 2016. Mitochondrial selfish elements and the evolution of biological novelties. Curr Zool 62:687–97.

Milani L, Ghiselli F, Pecci A, Maurizii MG, Passamonti M. 2015. The Expression of a Novel Mitochondrially-Encoded Gene in Gonadic Precursors May Drive Paternal Inheritance of Mitochondria. PLoS One 10:e0137468.

Milani L, Pecci A, Ghiselli F, Passamonti M, Bettini S, Franceschini V, Maurizii MG. 2017. VASA expression suggests shared germ line dynamics in bivalve molluscs. Histochem Cell Biol 148:157–71.

Milani L, Pecci A, Ghiselli F, Passamonti M, Lazzari M, Franceschini V, Maurizii MG. 2018. Germ cell line during the seasonal sexual rest of clams: finding niches of cells for gonad renewal. Histochem Cell Biol 149:105–10.

Mishra P, Chan DC. 2014. Mitochondrial dynamics and inheritance during cell division, development and disease. Nat Rev Mol Cell Biol 15:634–46.

Mitchell A, Guerra D, Stewart D, Breton S. 2016. In silico analyses of mitochondrial ORFans in freshwater mussels (Bivalvia: Unionoida) provide a framework for future studies of their origin and function. BMC Genomics 17:597.

Müller M, Mentel M, van Hellemond JJ, Henze K, Woehle C, Gould SB, Yu R-YY, van der Giezen M, Tielens AGM, Martin WF. 2012. Biochemistry and evolution of anaerobic energy metabolism in eukaryotes. Microbiol Mol Biol Rev 76:444–95.

Ninomiya Y, Ichinose S. 2007. Subcellular distribution of mitochondrial ribosomal RNA in the mouse oocyte and zygote. PLoS One 2:e1241.

Obata M, Komaru A. 2005. Specific location of sperm mitochondria in mussel *Mytilus*

galloprovincialis zygotes stained by MitoTracker. Dev Growth Differ 47:255–63.

Passamonti M, Ghiselli F. 2009. Doubly uniparental inheritance: two mitochondrial genomes, one precious model for organelle DNA inheritance and evolution. DNA Cell Biol 28:79–89.

Pozzi A, Plazzi F, Milani L, Ghiselli F, Passamonti M. 2017. SmithRNAs: Could Mitochondria “Bend” Nuclear Regulation? Mol Biol Evol 34:1960–73.

Punzi E, Milani L, Ghiselli F, Passamonti M. 2018. Lose it or keep it: (how bivalves can provide) insights into mitochondrial inheritance mechanisms. J Exp Zool B Mol Dev Evol 330:41–51.

Radzvilavicius AL, Blackstone NW. 2015. Conflict and cooperation in eukaryogenesis: implications for the timing of endosymbiosis and the evolution of sex. J R Soc Interface 12:20150584.

Reunov A. 2004. Is there a germ plasm in mouse oocytes? Zygote 12:329–32.

Reunov A, Alexandrova Y, Reunova Y, Komkova A, Milani L. 2019. Germ plasm provides clues on meiosis: the concerted action of germ plasm granules and mitochondria in gametogenesis of the clam *Ruditapes philippinarum*. Zygote 27:25–35.

Reunov A, Isaeva V, Au D, Wu R. 2000. Nuage constituents arising from mitochondria: is it possible? Dev Growth Differ 42:139–43.

Rossignol R, Faustin B, Rocher C, Malgat M, Mazat J-P, Letellier T. 2003. Mitochondrial threshold effects. Biochem J 370:751–62.

Sharpley MS, Marciniak C, Eckel-Mahan K, McManus M, Crimi M, Waymire K, Lin CS, Masubuchi S, Friend N, Koike M, Chalkia D, MacGregor G, Sassone-Corsi P, Wallace DC. 2012. Heteroplasmy of mouse mtDNA is genetically unstable and results in altered behavior and cognition. Cell 151:333–43.

Skibinski DOF, Ghiselli F, Diz AP, Milani L, Mullins JGL. 2017. Structure-Related Differences between Cytochrome Oxidase I Proteins in a Stable Heteroplasmic Mitochondrial System. Genome Biol. Evol. 9:3265–81.

Sokolova I. 2018. Mitochondrial Adaptations to Variable Environments and Their Role in Animals’ Stress Tolerance. Integr Comp Biol 58:519–31.

Solana J. 2013. Closing the circle of germline and stem cells: the Primordial Stem Cell hypothesis. Evodevo 4:2.

Stewart JB, Chinnery PF. 2015. The dynamics of mitochondrial DNA heteroplasmy: implications for human health and disease. Nat Rev Genet 16:530–42.

Sutovsky P, Moreno RD, Ramalho-Santos J, Dominko T, Simerly C, Schatten G. 2000. Ubiquitinated sperm mitochondria, selective proteolysis, and the regulation of mitochondrial inheritance in mammalian embryos. Biol Reprod 63:582–90.

Wang Z, Zou Y, Li X, Zhang Q, Chen L, Wu H, Su D, Chen Y, Guo J, Luo D, et al. 2006. Cytoplasmic male sterility of rice with boro II cytoplasm is caused by a cytotoxic peptide and is restored by two related PPR motif genes via distinct modes of mRNA silencing. Plant Cell 18:676–87.

White DJ, Wolff JN, Pierson M, Gemmell NJ. 2008. Revealing the hidden complexities of mtDNA inheritance. Mol Ecol 17:4925–42.

Wilding M, Carotenuto R, Infante V, Dale B, Marino M, Di Matteo L, Campanella C. 2001. Confocal microscopy analysis of the activity of mitochondria contained within the “mitochondrial cloud” during oogenesis in *Xenopus laevis*. Zygote 9:347–52.

Woloszynska M. 2010. Heteroplasmy and stoichiometric complexity of plant mitochondrial genomes--though this be madness, yet there’s method in't. J Exp Bot 61:657–71.

Zhang Y-Z, Ouyang Y-C, Hou Y, Schatten H, Chen D-Y, Sun Q-Y. 2008. Mitochondrial behavior during oogenesis in zebrafish: A confocal microscopy analysis: Mitochondrial behavior during oogenesis. Dev Growth Differ 50:189–201.

Zhou Q, Li H, Li H, Nakagawa A, Lin JLJ, Lee E-S, Harry BL, Skeen-Gaar RR, Suehiro Y, William D, Mitani S, Yuan HS, Kang B-H, Xue D. 2016. Mitochondrial endonuclease G mediates breakdown of paternal mitochondria upon fertilization. Science 353:394–99.

Zhou RR, Wang B, Wang J, Schatten H, Zhang YZ. 2010. Is the mitochondrial cloud the selection machinery for preferentially transmitting wild-type mtDNA between generations? Rewinding Müller’s ratchet efficiently. Curr Genet 56:101–7.

Zouros E. 2013. Biparental Inheritance Through Uniparental Transmission: The Doubly Uniparental Inheritance (DUI) of Mitochondrial DNA. Evol Biol 40:1–31.

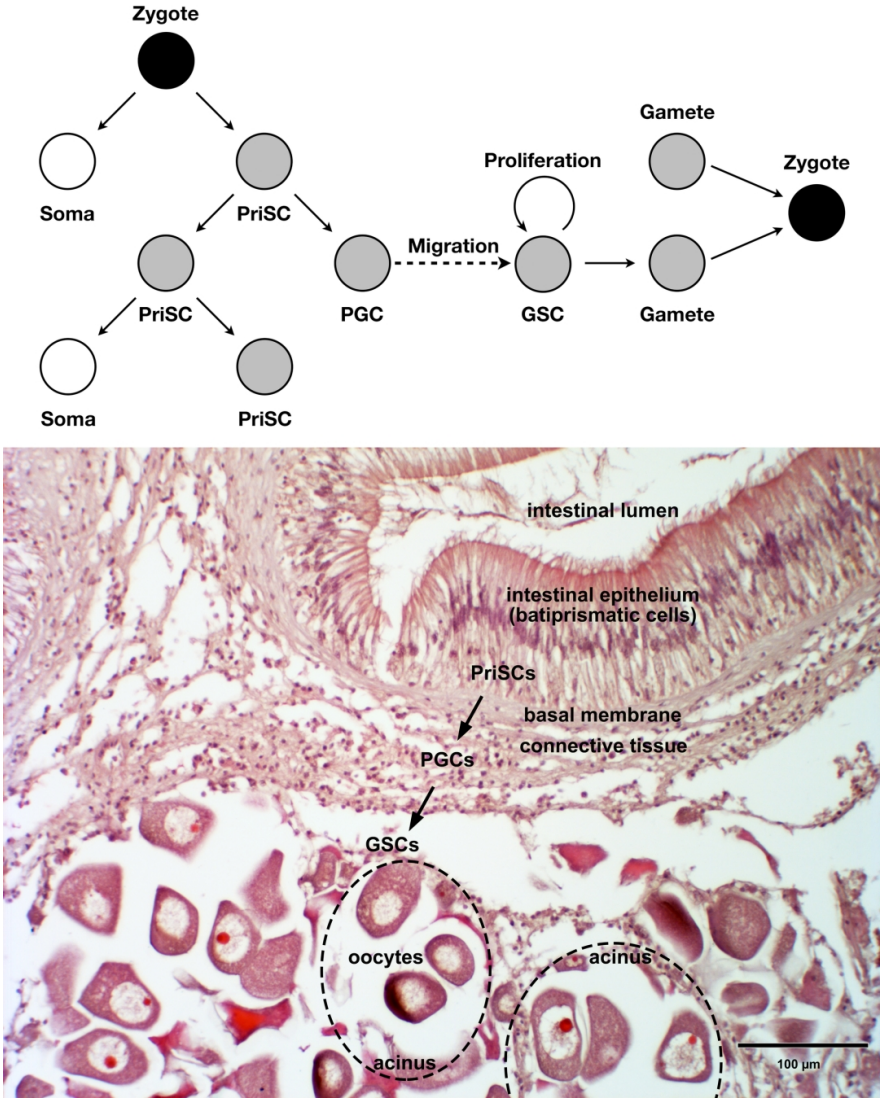

Fig. 1. Germline formation in R. philippinarum. A: The scheme represents the suggested process of germline differentiation based on the results previously obtained on the species (Milani et al. 2017, 2018). Primordial Stem Cells (PriSCs); Primordial Germ Cells (PGCs); Germinal Stem Cells (GSCs). B: Histological view of a female sample with indication about the localization of germ cell types. Hematoxylin and eosin staining following the method in Bettini et al. (2012).

170x216mm (300 x 300 DPI)

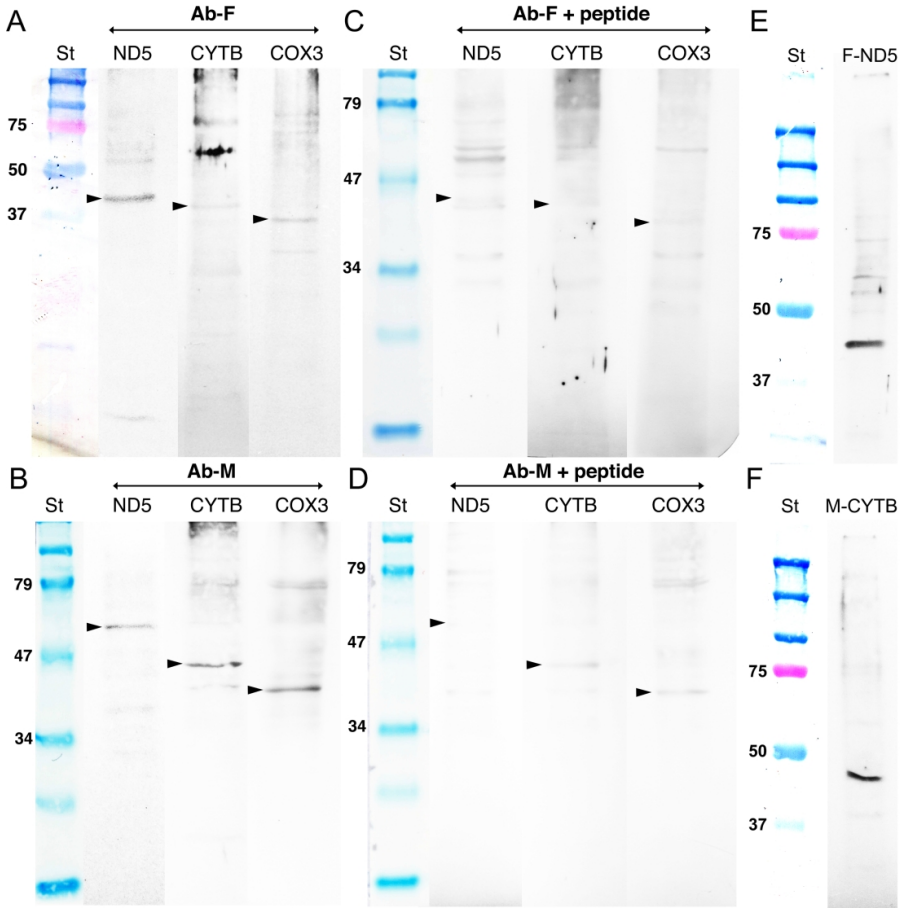

Fig. 2. Western blot. Western Blot of female and male gonadic extracts using anti-F and anti-M-type antibodies, respectively. Numbers indicate the molecular weight in kilodaltons of the adjacent band. Molecular weight standard lanes (St). The standards used are: Bio-Rad Precision Plus Protein™ Dual Color Standards (with a band of 75 kDa, pink) or Bio-Rad Prestained SDS-PAGE Standard Broad Range™. The bands detected with the three Ab-F (A) and the three Ab-M (B) are indicated by an arrowhead. A clear reduction of these F and M bands is visible in WB in which the anti-F-type (C) and the anti-M-type (D) antibodies are utilized after incubation with the corresponding synthetic peptide at a concentration of at least 10X compared to that of the primary antibodies. E,F) Example of WB optimization obtained for a couple of antibodies used in the double staining. F-ND5 lane, F-type antibody on female homogenate (RIPA buffer Ab1 1: 5,000). M-CYTB lane, M-type antibody on male homogenate (RIPA buffer; Ab1 1: 500 in 1% dried skimmed milk). Other details for antibody production and usage are reported in Suppl. Fig. 1 and Suppl. Table 1.

134x131mm (600 x 600 DPI)

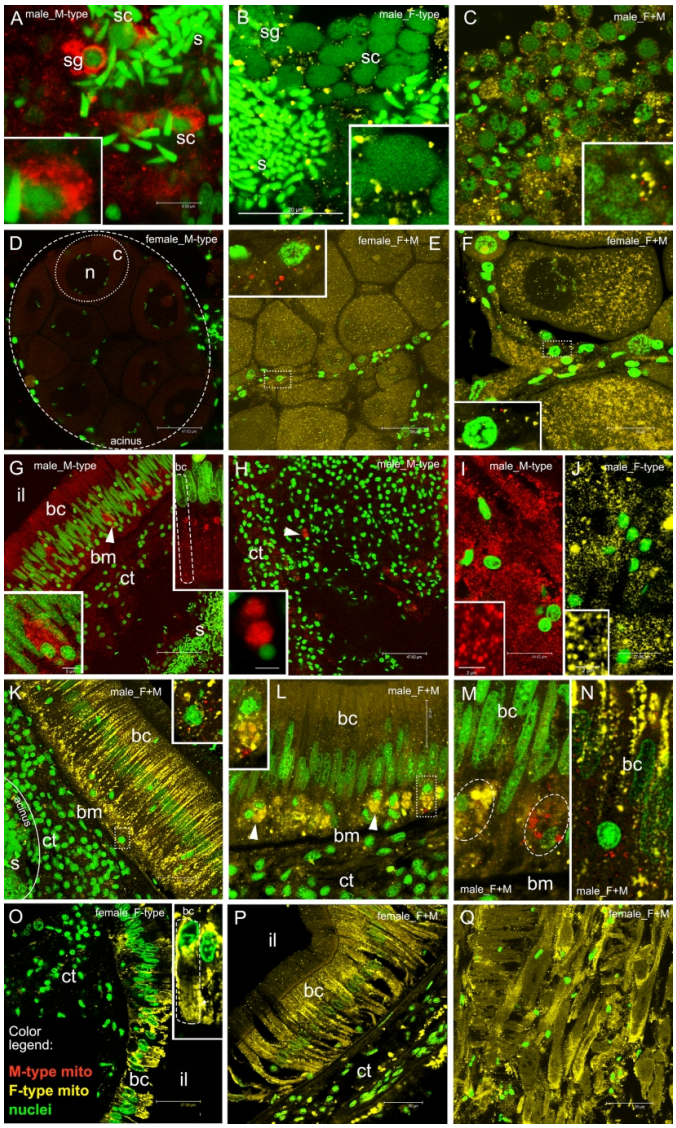

Fig. 3. Immunolocalization of M- and F-type mitochondrial proteins in germ cells (A-F) and in somatic tissues (G-Q) of R. philippinarum at confocal microscope.
Colors: anti-M-type, red; anti-F-type, yellow; TO-PRO®-3 nuclear dye, green.
Abbreviations in alphabetical order: batiprismatic cells of the intestinal epithelium, bc; basal membrane, bm; cytoplasm, c; connective tissue cells, ct; intestinal lumen, il; muscle cells, mc; nucleus, n; spermatozoa, s; spermatocytes, sc; spermatogonia, sg. PriSCs indicated by arrowhead. Differentiating germ cells show in the cytoplasm mitochondrial-size spots stained with one or the other type of antibody. A-C: Male germ cells. A: Anti-M antibody staining. In sc and sg. B: Anti-F antibody. In male germ cells. C: Anti-M/-F antibody double staining. In male germ cells. D-F: Female germ cells. D: Anti-M antibody staining. No staining is observed in late oocytes (one is circled in dotted line; chromosomes are visible at the periphery of n). E, F: Anti-M/-F antibody double staining. Only F-type mitochondria are visible in late oocytes. Both anti-M and anti-F stained spots are present in early germ cells at the periphery of the acini (early germ cells magnified in the insets). G-N: Male soma. G-I: Anti-M antibody staining. G: In ct, in bc (top right inset) and in putative PriSCs (lower left inset). H: Low labelling in ct and strong labelling in PriSCs (inset). I: In some males, mc

are strongly labelled with M-type antibody. J: Anti-F antibody. In other males, mc are F-type antibody labelled. K-N: Anti-M/-F antibody double staining. K, L: F-type mitochondria in bc; low F-type staining in ct. At higher magnification, a clear double staining is visible in PriSCs located close to bm (insets). M: Two PriSCs (circled) near bm with a prevalence of yellow (on the left) or red spots (on the right). N: A prevalent F-type staining is visible in bc, while some PriSCs (one shown) show a prevalence of M-type staining. O-Q: Female somatic tissues. O: Anti-F antibody. Present in ct and bc. P, Q: Anti-M/-F antibody double staining. P: Only F-type mitochondria in ct and bc. Q: Only F-type mitochondria in mc. See also Suppl. Figs. 2,3 and Suppl. Table 2.

160x267mm (300 x 300 DPI)

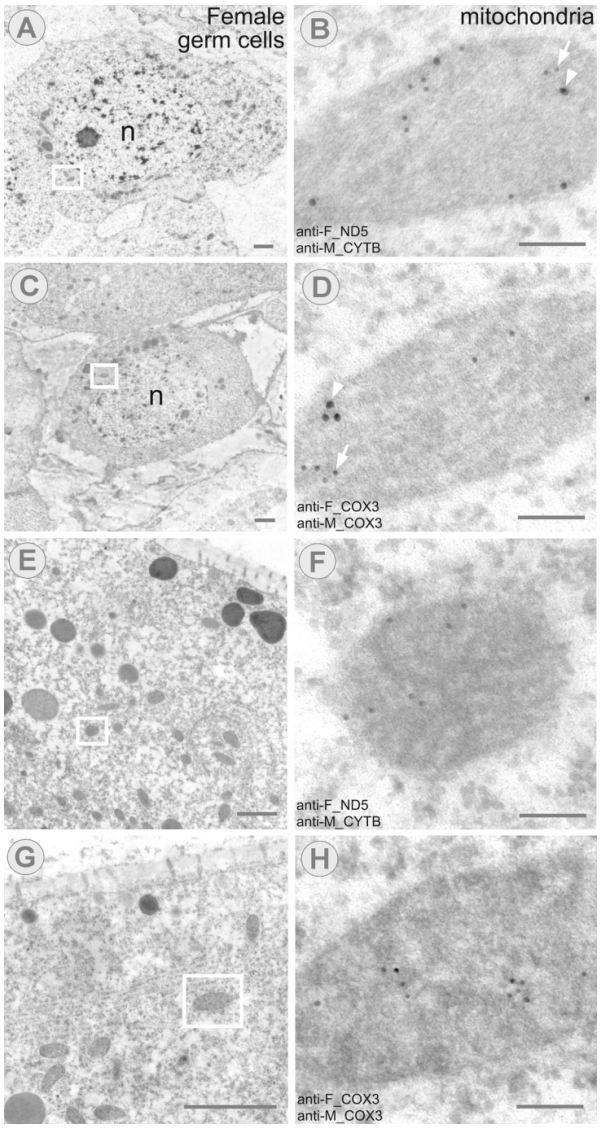

Fig. 4. Female germline of R. philippinarum with double immunostaining at TEM. A,B and E,F: anti-F_ND5 (12 nm) and anti-M_CYTB (18 nm). C,D and G,H: anti-F_COX3 (12 nm) and anti-M_COX3 (18 nm). Early germ cells (A,C) have mitochondria with both types of labelling (F- and M-type); B,D: magnification of the mitochondria in the white boxes in A and C, respectively (12 nm and 18 nm dots, arrow and arrowhead, respectively). Late oocytes (portions in E,G) have mitochondria with only F-type labelling (12 nm) (F,H: magnification of the mitochondria in the white boxes in E and G, respectively). Nuclei, n. Scale bars: left column 2 µm; right column 0.2 µm.

89x167mm (300 x 300 DPI)

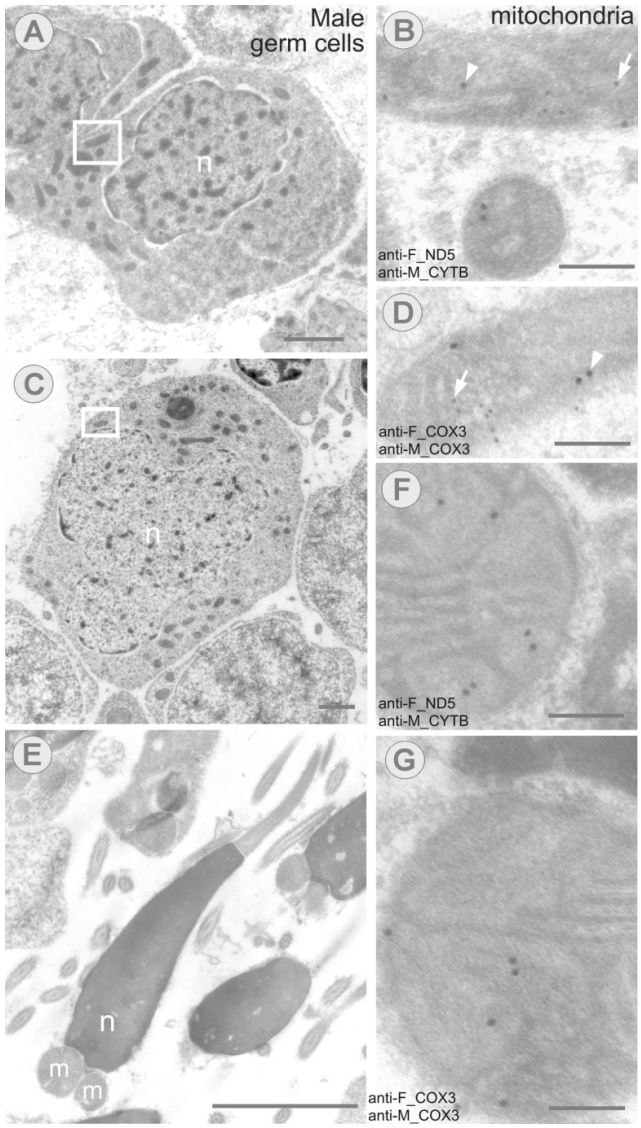

Fig. 5. Male germline of R. philippinarum with double immunostaining at TEM.
A,B and F: anti-F_ND5 (12 nm) and anti-M_CYTB (18 nm). C,D and G: anti-F_COX3 (12 nm) and anti-M_COX3 (18 nm). Early germ cells (A,C) have mitochondria with both types of labelling (F- and M-type); B,D: magnification of the mitochondria in the white boxes in A and C, respectively) (12 nm and 18 nm dots, arrow and arrowhead, respectively). Spermatozoa (E) have mitochondria (m) with only M-type labelling (18 nm), magnified in (F,G). Nuclei, n. Scale bars: left column 2 μm; right column 0.2 μm.

88x157mm (300 x 300 DPI)

Supplementary Table 1. Characteristics of primary antibodies and OXPHOS proteins
Expected reactivity (*in silico* calculation) of the antibodies and the dilutions used in Western blot and immunohistochemistry. OXPHOS protein expected and obtained molecular weight.

Expected reactivity (*in silico* calculation)					
					doub e mmuno
Protein	**Peptide**	**Antigenicity**	**Solubility**	**Epitope**	
	n rabb t				
Rph F ND5	LWQSGVKNMFMGMSNKVLK	med um	med um	med um	X
Rph F CYTB	YNVVSITSGFSSHSLK	med um	ow	med um	
Rph F COX3	FFHSEMGDMVPLLMGLS	ow	ow	med um	X
Protein	**Peptide**	**Antigenicity**	**Solubility**	**Epitope**	
	n ch cken				
Rph M ND5	FIGSKVINSISMVFRNKIWE	ow	med um	med um	
Rph M CYTB	LWEKVSKNVEKKVEK	good	good	good	X
Rph_M_COX3	YFSIFILVHSIIS	ow	ow	med um	X
Concentration in Western Blot and Immunohistochemistry					
Protein	**Peptide**	**Wetern Blot**	**WB optimized (*)**	**Immuno**	**Immuno opt**
	n rabb t				
Rph F ND5	LWQSGVKNMFMGMSNKVLK	1:100 – 1:100000	1:200-5,000(+2%dsm)	1:20 – 1:10000	1:200
Rph F CYTB	YNVVSITSGFSSHSLK	1:100 – 1:100000	1:200+2%dsm	1:20 – 1:10000	1:30
Rph F COX3	FFHSEMGDMVPLLMGLS	1:100 – 1:100000	1:200+2%dsm	1:20 – 1:10000	1:100
Protein	**Peptide**	**Wetern Blot**	**WB optimized (*)**	**Immuno**	**Immuno opt**
	n ch cken				
Rph M ND5	FIGSKVINSISMVFRNKIWE	1:100 – 1:100000	1:250+1%dsm	1:20 – 1:10000	1:200
Rph_M_CYTB	LWEKVSKNVEKKVEK	1:100 – 1:100000	1:500+1%dsm	1:20 – 1:10000	1:300
Rph M COX3	YFSIFILVHSIIS	1:100 – 1:100000	1:250+1%dsm	1:20 – 1:10000	1:150
OXPHOS protein molecular weight					
Protein	**length AA**	**kDa calculated (**)**	**kDa obtained (WB)**		
Rph F ND5	542	60.47 - 60.46	~45		
Rph F CYTB	416	46.57 - 46.56	~44		
Rph_F_COX3	292	34.04 - 34.03	~37		
Protein	**length AA**	**kDa calculated (**)**	**kDa obtained (WB)**		
Rph_M_ND5	563	62.78 - 62.78	~62		
Rph M CYTB	441	49.61 - 49.60	~46		
Rph M COX3	298	34.57 - 34.56	~40		

Note: (*) for 30-40 µg; (**) http://www.b o nformat cs.org/sms/prot_mw.htm - http://web.expasy.org/compute_p /; engthAA: from GenBank annotat on; dsm = dr ed sk mmed m k.

Supplementary Table 2. Summary of the localization of anti-OXPHOS staining in female and male tissues

	undifferentiated/ early germ cells	oocytes	spermatozoa	batiprismatic cells (gut)	connective tissue	muscle cells	PriSCs	PGCs/GSCs
F-TYPE								
Anti-F_ND5								
females	X	X		X	X		X	X
males				X	X			
Anti-F_CYTB								
females	X	X			X		X	X
males	X			X	X	X	X	X
Anti-F_COX3								
females	X	X		X	X		X	X
males	X					X		
M-TYPE								
Anti-M_ND5								
females	X						X	X
males	X		X					
Anti-M_CYTB								
females	X						X	X
males	X		X	X			X	
Anti-M_COX3								
females	X						X	X
males	X		X	X	X	X	X	X

Supplementary Fig. 1.
Alignments of F- and M-type of mitochondrial proteins (ND5, CYTB and COX3).
The peptides used for immunization and antibody production are in green.
The "disagreements" in amino acids between the two aligned sequences are in colors.

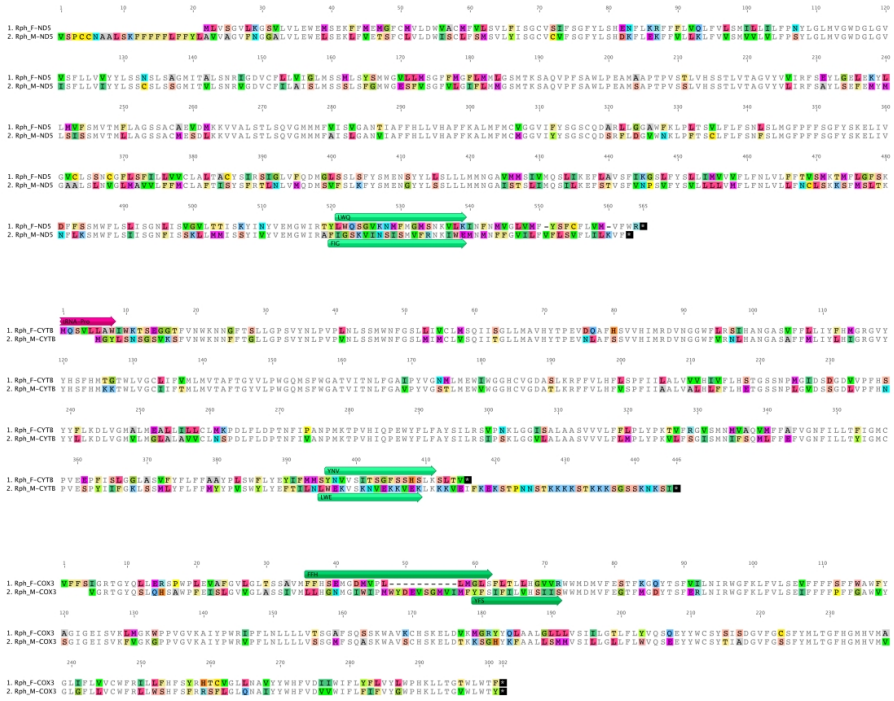

209x192mm (600 x 600 DPI)

Supplementary Fig. 2.
Control sections for the immunological analyses in which the primary antibodies were omitted (-Ab1).
A: Female section of a portion of gonadic and connective tissues with only secondary anti-M antibody (DyLight 550). No staining is present in oocytes at different stages of differentiation (dotted circles) (c: cytoplasm; n: nucleus) inside an acinus (dashed oval) and in the somatic cells of the connective tissue (ct; lower left).
B: Female section of a portion of gonadic and connective tissues (ct) with secondary anti-F antibody (Alexa Fluor 488). No staining is present in late and early oocytes (dotted circles) inside an acinus (dashed oval) and in the cells localized at the acinus wall.
C-D: Female sections of a portion of intestinal epithelium (batiprismatic cells, bc) and adjacent connective tissue (ct) with anti-M secondary antibody (DyLight 550) (**C**), and anti-F secondary antibody (Alexa Fluor 488) (**D**). With both the antibodies, no staining is evident in batiprismatic cells and in the connective cells. The slight marking observed in Primordial Stem Cells (PriSCs) located in the intestinal epithelium near the basal membrane (bm) can be considered not significant if compared to that obtained with the corresponding primary antibodies (see the main text).
Red: Ab2 M; yellow: Ab2 F; green: TO-PRO®-3 nuclear dye.

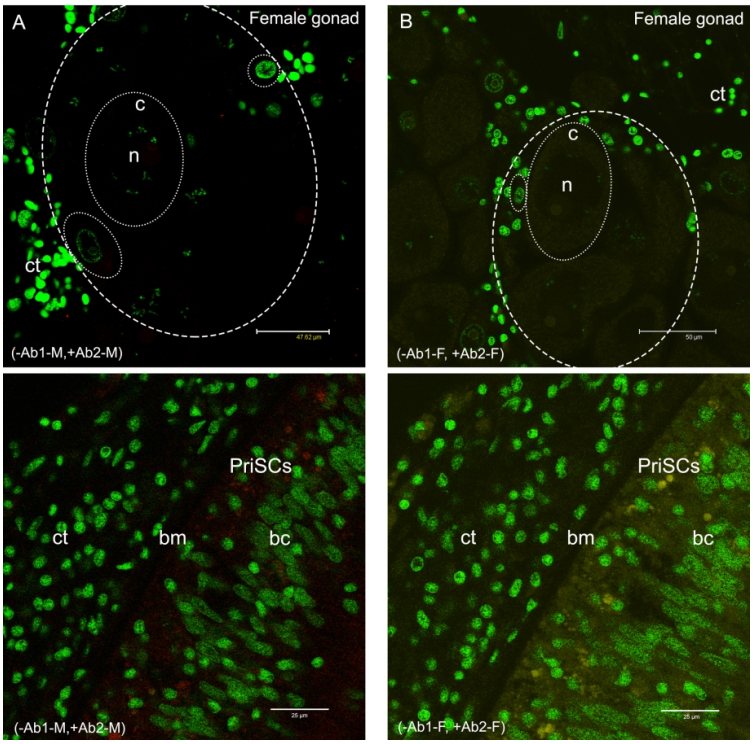

183x274mm (300 x 300 DPI)

Supplementary Fig. 3.
Schematic representation of mitochondrial segregation during germline differentiation in the DUI species *R. philippinarum*.
Simplification of the hypothesized process leading to homoplasmic gametes. While Primordial Stem Cells (PriSCs) appear to contain both the types of mitochondria (F and M), during germ cell differentiation there is the loss of the non sex-specific mitochondrial type. Primordial Germ Cells (PGCs); Germinal Stem Cells (GSCs); batiprismatic cells of the intestinal epithelium (BC); basal membrane (BM).
Red: M-type mitochondria; yellow: F-type mitochondria; green: nuclei.

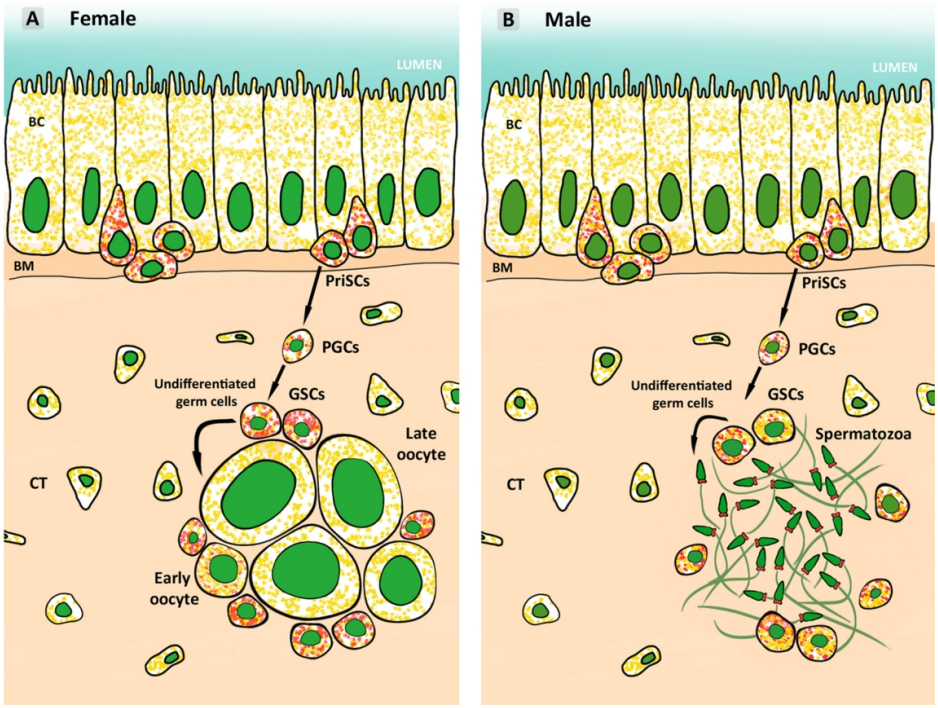

170x167mm (300 x 300 DPI)